Proc. CIBSE A: Building Serv. Eng. Res. Technol. 21(1) 53–61 (2000) Printed in Great Britain B595

Summary A simulation model of a discharge air temperature plant is developed using SIMULINK within the MATLAB environment. Step response results from an open-loop form of this model are correlated with experimental data with good agreement. Settings for a fixed-parameter PID controller are 'benchmarked' from manufacturers' recommendations and optimised at local plant operating conditions using cost-function minimisation. A closed-loop form of the plant model is simulated using these controller specifications, revealing significant lack of robustness due to plant nonlinearity when the manufacturers' recommendations were applied. The locally optimised PID controller performed well, but this would require extensive understanding of plant characteristics to be achieved in practice. In a second part of this paper, a method is developed that achieves robust control for a wide variety of plant operating conditions based on simple *a priori* data about the plant.

Robust control of HVAC plant I: modelling

C P Underwood BSc PhD CEng MCIBSE MASHRAE
School of the Built Environment, University of Northumbria, Ellison Place, Newcastle upon Tyne NE1 8ST, UK

Received 27 October 1999, in final form 24 February 2000

List of symbols

t	Time (s)
θ	Temperature (K, °C)
m	Mass flow rate (kg s^{-1})
q	Heat transfer rate (W)
c	Specific heat capacity (J kg^{-1} K^{-1})
C	Thermal capacity (J K^{-1})
U	Thermal transmission coefficient (W $m^{-2}K^{-1}$)
Nu	Nusselt number
Re	Reynolds number
Pr	Prandtl number
A	Surface area (m^2)
D	Diameter (m)
k	Thermal conductivity (W $m^{-1}K^{-1}$)
v	Velocity (m s^{-1})
ρ	Density (kg m^{-3})
μ	Viscosity (kg $m^{-1}s^{-1}$)
τ	Time constant (s)
d_p	Delay time (s)
d_i	Internal tube diameter (m)
ϕ	Detector output or feedback signal (°C)
r	Reference or set point (°C)
u	Control signal
n	Integer number
γ	Valve inherent characteristic
ψ	Valve installed characteristic
f_o	Valve let-by
N	Valve authority
K	Gain (K^{-1})
I	Controller integral time (s)

Subscripts

a	Air
w	Water
ai	Air inlet side
ao	Air outlet side
wi	Water inlet side
wo	Water outlet side
m	Metal
wd	Water–design condition
i	Internal
t	Tube
d	Detector
c	Controller
p	Plant

1 Introduction

In this work, the robust control of a nonlinear HVAC plant is considered. Recent work has addressed the problem of controlling plants experiencing nonlinearity and multiple operating modes using adaptive control (for example, references 1 to 4). Many of these solutions have lacked robustness when something 'unexpected' happens. Other recent work has explored the use of fuzzy logic control and artificial neural networks (ANNs) (for example, references 5 to 8). However, these methods are difficult to implement; fuzzy control requires experiential knowledge and qualitative data about plant operation and response that are often unavailable or difficult to obtain. Successful ANN design requires extensive training data that are often difficult to obtain. It is argued that robust fixed-parameter control offers a convenient and simple alternative to achieving stable feedback control with at least reasonable performance across all expected modes of plant operation.

Thus the objectives of this work are:

— to develop a simulation model of a typical HVAC plant and establish a 'benchmark' controller

— to use results from the simulation to establish an uncertain linear plant model

— to design a robust fixed-parameter controller based on a weighted form of the uncertain plant model, comparing its performance with the benchmark controller.

Part I deals with the simulation modelling and benchmark controller development. Part II deals with the design and implementation of the robust controller.

The plant considered is a common example in HVAC control, used for the hot water heating of fresh air to a controlled downstream duct temperature (Figure 1). It is emphasised that this plant is merely an exemplar—the methods developed, especially in Part II, have considerable generality for this general class of plant.

Section 2 reviews previous work in modelling HVAC plant with specific reference to control system synthesis and design. Section 3 deals with model development, and in section 4 the model is verified using experimental data based on step response tests. Section 5 deals with controller benchmarking,

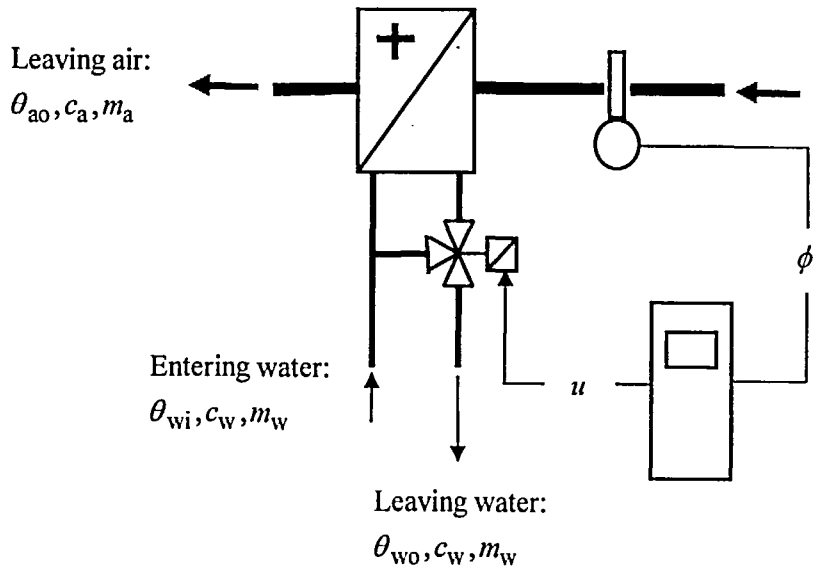

Figure 1 General discharge temperature control problem

and in section 6 closed-loop simulation results are obtained. Conclusions are drawn in section 7.

2 Modelling of HVAC plant for control synthesis

Adams and Holmes[9] first considered component model descriptions appropriate to HVAC control synthesis. Their work was restricted to linear transfer functions of key components in HVAC systems such as sensors, coils and heat emitters. Nevertheless, this work produced some of the first component-based models enabling stability and response analysis of HVAC systems.

The modelling of the discharge air temperature control problem with proportional-plus-integral (PI) control has been considered by Gondal[10], whose analysis was restricted to linear modelling around a finite operating range. Shavit and Brandt[11] developed a nonlinear model enabling conditions for satisfactory controller performance to be identified, and Borresen[12] considers steam-heated coils using an adaptive PI controller. Brath *et al*[13] go on to broaden the acceptable performance and stability range of the controller using gain-scheduling, which leads to improvements but depends on accurate plant identification. Recognising the limitations of purely theoretical modelling, there has also been some work done on empirical model-fitting for dynamic plant analysis[14,15], but these studies have tended to result in plant models that are problem-specific.

Developments in modular simulation programs have addressed problem-specificity; the two most promising developments are TRNSYS[16] and HVACSIM+[17]. Underwood, for instance, has developed HVAC control component models for TRNSYS that have general applicability[18], while HVACSIM+ has been used extensively for investigating a wide range of HVAC control problems[19,20]. One restriction with these modular programs is that many of the plant component models are steady-state or quasi-steady-state, making them suitable (and computationally efficient) for low-frequency dynamic analysis but unsuitable for high-frequency disturbances, which are important in many instances of control design.

It is therefore argued that a modelling environment is needed in which developed models have a high degree of transportability and transparency, and the model itself requires to be spectrally inclusive for wide applicability in control synthesis and design. A modelling environment that has the potential to meet these needs is MATLAB-SIMULINK[21], which has the added advantage of convenient access to a very wide range of control system analysis and design tools. Hence this method has been used in the present work.

3 Model development

A lumped-capacity approach has been adopted in which each heat exchange zone is assumed to behave as a 'continuously stirred tank'.

An energy balance on the water side gives

$$C_w \frac{d\theta_{wo}}{dt} = m_w c_w(\theta_{wi} - \theta_{wo}) - q_w \tag{1}$$

and for the coil and fin material

$$C_m \frac{d\theta_m}{dt} = q_w - q_a \tag{2}$$

in which the heat transfer rates are given by

$$q_a = U_a A_a(\theta_m - \theta_{ao}) \tag{3}$$

$$q_w = U_w A_w(\theta_{wo} - \theta_m) \tag{4}$$

If instantaneous heat exchange is assumed on the air side:

$$q_a = m_a c_a(\theta_{ao} - \theta_{ai}) \tag{5}$$

Combining equations 3 and 5:

$$\theta_{ao} = \frac{m_a c_a \theta_{ai} + U_a A_a \theta_m}{m_a c_a + U_a A_a} \tag{6}$$

For U_w, we can apply one of a number of forced surface convection correlations such as the Dittus–Boelter correlation[22]:

$$Nu_d = \frac{U_w d_i}{k_w} = 0.023\, Re^{0.8} Pr^{0.33} \tag{7}$$

in which

$$Re = \frac{\rho_w v_w d_i}{\mu_w} = \frac{4m_w}{n_t \mu_w \pi d_i} \quad (8)$$

Combining equations 7 and 8 leads to a more convenient interpretation of the Dittus–Boelter correlation from the modelling viewpoint, in which the water mass flow rate appears explicitly:

$$U_w = 0.0279 \times \left[\frac{Pr^{0.33} k_w}{\mu_w^{0.8}}\right] \times \left[\frac{m_w}{n_t d_i^{2.25}}\right]^{0.8} \quad (9)$$

Curve fitting to standard property tables[23] for water in the temperature range applicable to most practical hot water heating and chilled water cooling applications gives the following:

$$\frac{Pr^{0.33} k_w}{\mu_w^{0.8}} = 208.69 + 4.1317\theta_{wo} - 5.31 \times 10^{-3}\theta_{wo}^2 \quad (10)$$

Thus, combining equations 9 and 10:

$$U_w = (5.823 + 1.153 \times 10^{-1}\theta_{wo} - 1.48 \times 10^{-4}\theta_{wo}^2) \times \left[\frac{m_w}{n_t d_i^{2.25}}\right]^{0.8} \quad (11)$$

Equation 11 applies to turbulent forced convection ($Re > 2300$). During light load, the flow rate delivered by the control valve will reduce and there will be occasions when laminar forced convection is possible. In these conditions, Nu_d tends to a constant and may for practical purposes be taken as 4.36[24] such that, after applying a curve-fit function for the thermal conductivity of water,

$$U_w|_{Re<2300} = \frac{4.36}{d_i} \times (5.702 \times 10^{-1} + 1.79 \times 10^{-3}\bar{\theta}_{wm} - 6.7714 \times 10^{-6}\bar{\theta}_{wm}^2) \quad (12)$$

in which $\bar{\theta}_{wm}$ is the mean of the outlet water and heat exchanger material temperatures.

However, the transition between turbulent and laminar flow is gradual, whereas equations 11 and 12 imply a sharp edge. This was addressed by relaxing the transition between the two as follows:

$$U_w = \max(U_w|_{Re \geq 2300}, U_w|_{Re<2300}) \quad (13)$$

The effect of this is to over-estimate the water side heat transfer rate, but since $U_w >> U_a$ in general (i.e. the air side thermal resistance is dominant), this was not considered to have a significant impact on model accuracy.

To obtain U_a, tests were conducted on a laboratory-scale pilot rig (described in section 4). Inlet and outlet temperatures, water flow rates and air flow rates were recorded with the rig operating at steady state but at five different water flow rates and, hence, different coil capacities. From the overall heat transfer rates at these conditions, the overall coil U-value was found from a knowledge of the heat exchanger surface area. Then, using either equation 11 or 12 for the appropriate water flow conditions, the air side U-value was expressed. From these results, it was clear that the air side U-value was strongly dependent on the heat exchanger material temperature, θ_m, see Figure 2. The rationale behind this is as follows. The air

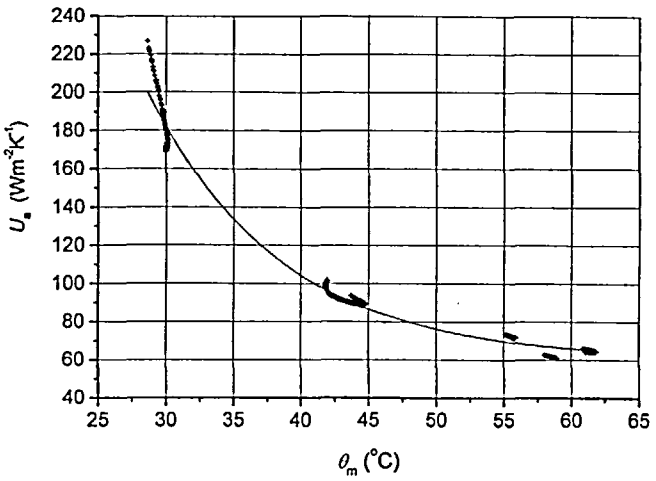

Figure 2 Air side U-value

velocity across the tube/fin combination is well understood to be in the laminar region (see, for example, Gomaa *et al*[25]). Under such conditions, the temperature gradient in the near-wall region is low and conduction mechanisms become dominant within the boundary layer. If the wall temperature is high in relation to the fluid mean bulk temperature (as it is in this case), it is reasonable to suppose that the wall temperature effect will dominate the heat transfer rate owing to its influence over fluid properties in the boundary layer.

The five clusters of points represent the various results gathered at each coil operating condition, the clusters themselves arising from minor variations in water inlet temperatures during rig operation. It was possible to fit the following exponential function to these data, thus providing an expression for the air side U-value:

$$U_a = 60.37 + 140.3 \times \exp\left[\frac{28.62 - \theta_m}{9.796}\right] \quad (14)$$

A sub-system dealing with heat transfer calculations can now be defined based on equations 11–14 (Figure 3).

A first-order representation was assumed for the control valve and actuator. Hysteresis due to the actuator linkage mechanism was assumed to be negligible in this application and was therefore neglected:

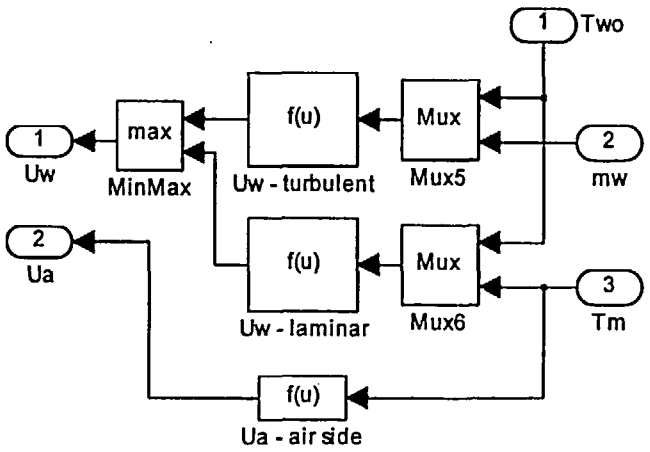

Figure 3 Heat transfer sub-system

$$\tau_a \frac{dm_w}{dt} = \psi m_{wd} - m_w \quad (15)$$

The normalised installed valve characteristic in the above, ψ, can be shown[26] to be

$$\psi = \gamma \times [\gamma^2 (1 - N) + N]^{-1/2} \quad (16)$$

in which the inherent valve characteristic, γ, will be

$$\gamma = f_o^{(1-u)} \quad \text{for an equal percentage valve} \quad (17)$$

and

$$\gamma = f_o + u(1 - f_o) \text{ for a linear valve} \quad (18)$$

The valve was interpreted as the sub-system of Figure 4.

A first-order representation was also assumed for the temperature sensor:

$$\tau_d \frac{d\phi}{dt} = \theta_{ao} - \phi \quad (19)$$

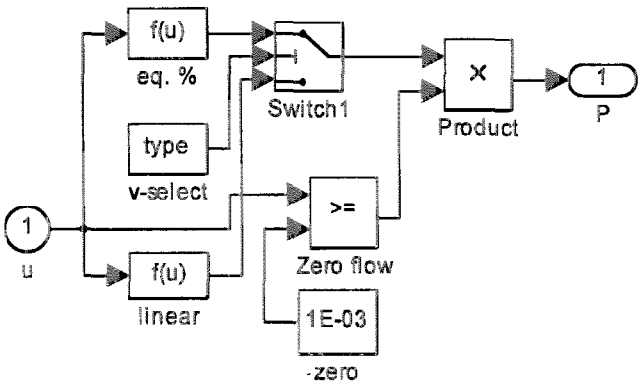

Figure 4 Valve sub-system

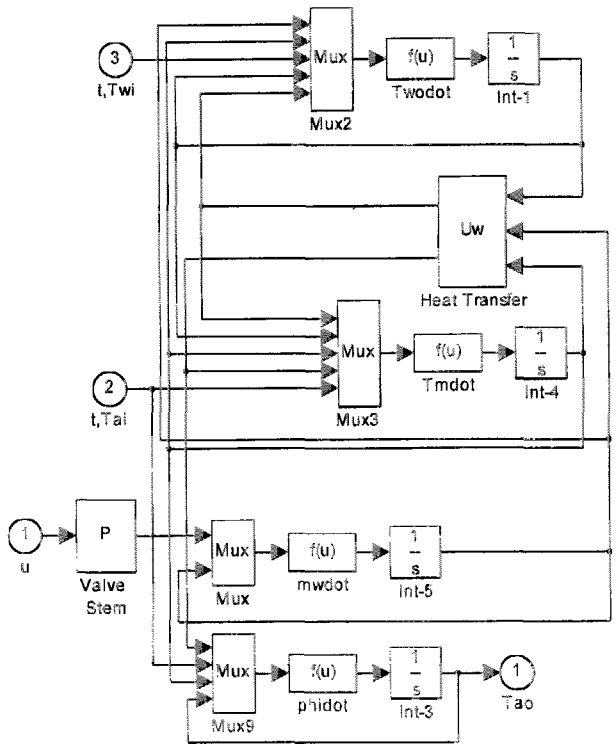

Figure 5 Open-loop plant model

The model was initially synthesised as an open-loop problem (Figure 5, showing the two sub-systems, inputs, constants and integrators). All differential equations are integrated using a standard fourth-order Runge–Kutta scheme.

Finally, the open-loop plant model is masked as a single block (Figure 6), with reference input, inlet air and water temperatures and output plotting device.

In summary, the open-loop model has 14 parameters:

$$C_w, c_w, A_w, C_m, A_a, c_p, f_o, N, m_{wd}, m_a, \tau_a, \tau_d, d_i, n_t$$

There are three inputs: θ_{wi}, θ_{ai}, u and four derivatives: θ_{wo}, θ_m, m_w, ϕ.

4 Model verification

The open-loop model was first applied to a laboratory pilot rig (Figure 7). Values for the model inputs, parameters and initial conditions are given in Table 1.

In Table 1, C_w, C_m, A_w, A_a, d_i and n_t were obtained from the two-row coil installed in the rig. C_w is based on the static water mass of the coil multiplied by the specific heat capacity of water (c_w) which was assumed constant. m_{wd}, m_a and N were obtained from measurements conducted on the rig at rated operating conditions. The valve constant f_o was taken from manufacturers' data for the three-port valve concerned and

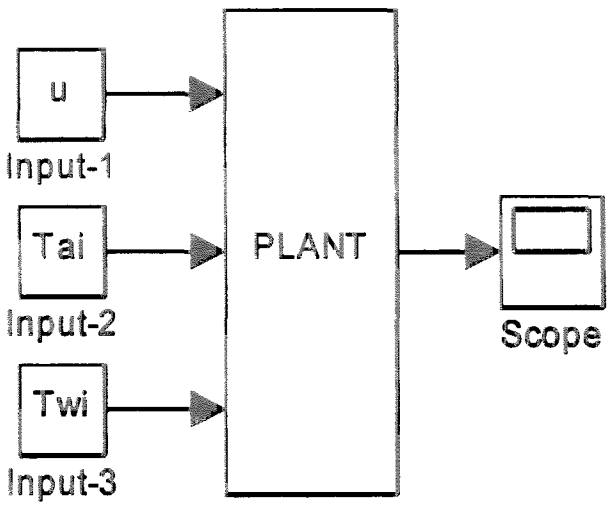

Figure 6 Masked plant model

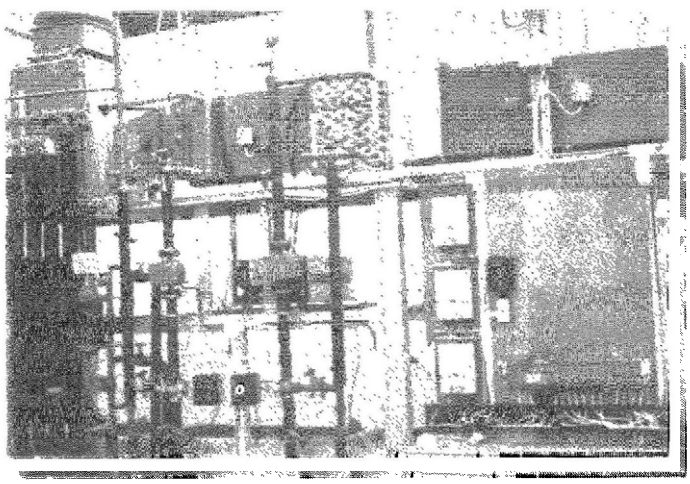

Figure 7 Laboratory pilot rig

Table 1 Model inputs

Model input	Value
Parameter C_w	4.836 kJ K^{-1}
Parameter C_m	4.047 kJ K^{-1}
Parameter A_w	0.404 m^2
Parameter A_a	5.181 m^2
Parameter c_w	4.194 kJ $kg^{-1}K^{-1}$
Parameter c_a	1.002 kJ $kg^{-1}K^{-1}$
Parameter m_{wd}	0.619 kg s^{-1}
Parameter N	0.371
Parameter f_o	0.045
Parameter d_i	0.0117 m
Parameter n_t	10
Parameter τ_a	26.7 s
Parameter τ_d	30 s
Parameter m_a	0.3144 kg s^{-1}
Initial condition $\theta_{ao}(0)$	$\theta_{ai}(0)$
Initial condition $\theta_m(0)$	$\theta_{ai}(0)$
Initial condition $m_w(0)$	0
Initial condition $\phi(0)$	$\theta_{ai}(0)$

the time constants τ_a, τ_d were obtained from observations made on the plant.

Five step response tests were conducted on the rig in which the valve input signal, u, was stepped from an initial zero state to 0.2, 0.4, 0.6, 0.8 and 1 (full travel) respectively. These patterns of u, together with the measured time series of the boundary variables $\theta_{ai}(t)$, $\theta_{wi}(t)$ were used as inputs to the open-loop model. Time series results of the leading output variable of interest, $\theta_{ao}(t)$, generated by the model and measured from the rig for the various u input patterns are compared in Figures 8a–e. In general, it can be seen that the model gives good results when compared with experimental data from the pilot rig, the root-mean-square (RMS) error being 1.96 K, 1.19 K, 1.42 K, 1.29 K and 1.73 K, respectively, giving an overall mean RMS error of 1.5 K for all results.

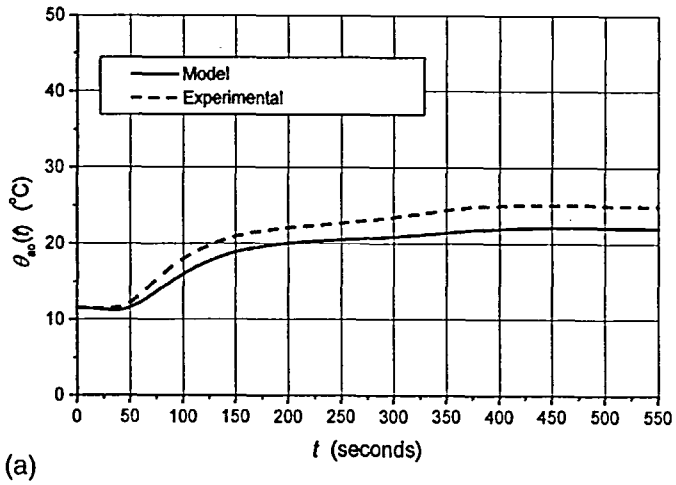

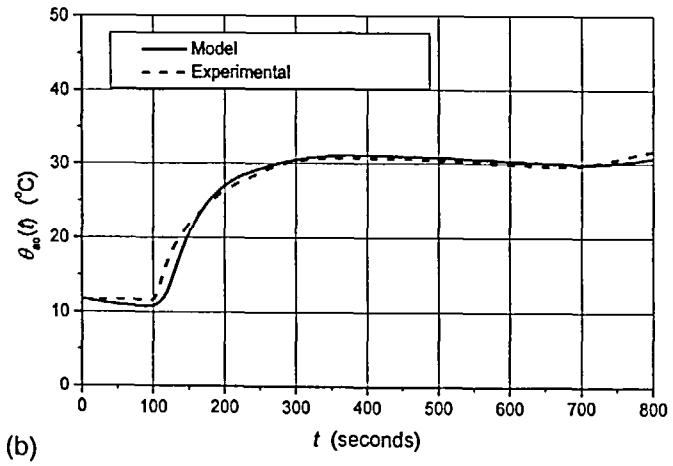

Figure 8 (a) 20% step response test results. (b) 40% step response test results. (c) 60% step response test results. (d) 80% step response test results. (e) 100% step response test results

5 Controller benchmarking

Current practice for the control of the plant considered in the present work would be to close a feedback loop with some combination of proportional-plus-integral-plus-derivative (PID) controller. A survey of four leading HVAC control suppliers was carried out to establish what combination of

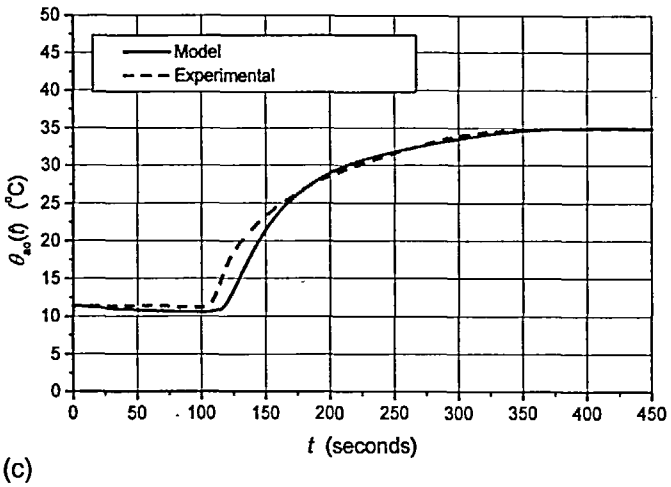

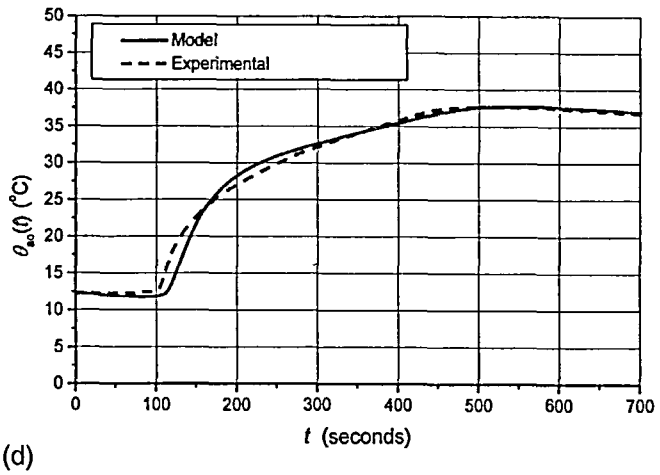

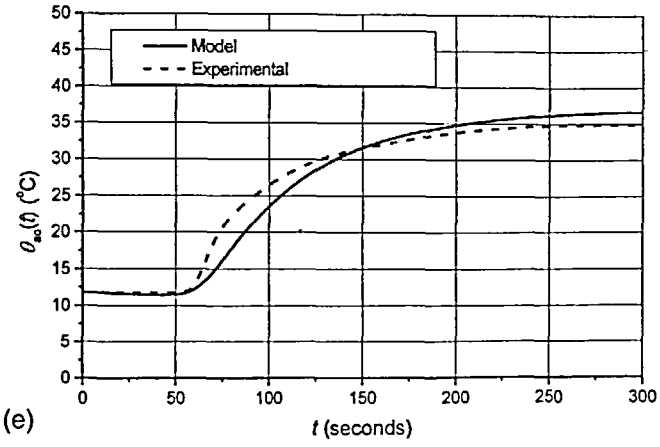

control actions would be used and what, if any, arrangements would be made for adjustments of the control system once installed. All four suppliers were consistent in that for this application they would specify a PID controller but would only adopt the proportional and integral terms (i.e. PI control only would be used). All suppliers indicated nominal or 'first approximations' for the settings of the proportional and integral terms. Three of the suppliers confirmed that these would form the basis of further on-site adjustment if necessary, while the other supplier commented that the 'factory' settings used in his controller would not normally require further adjustment on site. The results of the short survey are summarised below.

Supplier A
- Product: universal single output HVAC controller
- Nominal proportional band: 50%
- Nominal integral action time: 10 min
- Derivative action time: 0 min

Supplier B
- Product: general PID controller for HVAC applications
- Nominal proportional band: 20%
- Nominal integral action time: 10 min
- Derivative action time: 0 min

Supplier C
- Product: single output air handling supply temperature controller
- Nominal proportional band: 40% ('factory' setting)
- Nominal integral action time: 3 min ('factory' setting)
- Derivative action time: 0 min ('factory' setting)

Supplier D
- Product: DDC universal HVAC controller
- Nominal proportional band: 16%
- Nominal integral action time: 3 min
- Derivative action time: 0 min

It is convenient from the modelling viewpoint to express the controller gain with respect to an applied temperature error input and a controller output in the interval 0–1. Thus the feedback controller settings values of the four suppliers range from a most cautious gain and integral time of 0.08 K^{-1} and 10 min, respectively, to a least cautious 0.25 K^{-1} and 3 min, based on a controlled temperature range for this plant of 25 K.

The open-loop model of Figure 6 was closed with a feedback loop and a PID controller whose nominal settings take on the values given above. The resulting closed-loop model is shown in Figure 9. The controller was configured using standard integrator and derivative blocks available within the program component library used (Figure 10), but the integrator block was configured with its output reset to zero during all plant-inactive periods in order to inhibit integral wind-up. This was achieved by providing the additional inputs of control reference (r) and inlet air temperature (θ_{ai}) to the controller model. When the plant is inactive, $r = \theta_{ai}$, and the relational operator 'fires' a zero, thus zeroing controller output (at all other times, $r \neq \theta_{ai}$, and the relational operator 'fires' 1).

It is possible to obtain optimum PI settings using the nominal values as a starting point by minimising a cost function attached to the target variable, $\theta_{ao}(t)$. This process is more or less equivalent to using an automated self-tuner on site. In practice, tuning will normally take place in the off-design when the plant is operating around the required set point but with higher entering air temperatures, simply because it will rarely be convenient to wait for design conditions to prevail before commissioning is carried out. The optimisation was

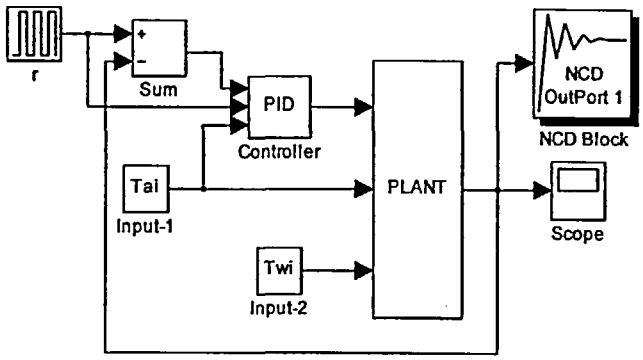

Figure 9 Closed-loop model

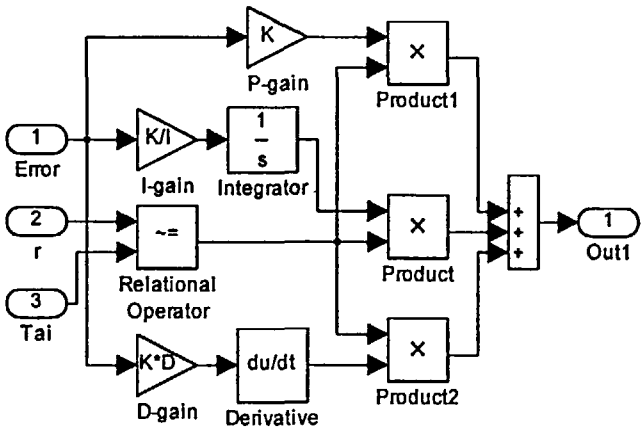

Figure 10 PID controller sub-system

therefore carried out using a nonlinear control design blockset available from within the extended program library used (NCD block in Figure 9) at an arbitrarily chosen mid-season condition corresponding to an entering air temperature of 8.5°C (equivalent to half design load).

The NCD block works as follows. A constraint envelope is defined that defines upper and lower bounds of the controlled variable, together with one or more tunable variables. A cost function is generated consisting of a weighted maximum constraint violation. At each iteration, each tunable variable is perturbed in turn and the resulting constraint values and cost function are evaluated. A gradient search direction is determined from these results and a line search along the gradient is performed in order to minimise the cost function while simultaneously satisfying the constraint envelope criteria.

Hence the NCD block setup involved the following:

- A constraint envelope was defined for the controlled variable, $\theta_{ao}(t)$. This consisted of an arbitrary but 'desirable' response to a step change in r from an initial 8.5°C ($t = 0$) to 22°C ($0 < t \leq 300$ s), settling at 20°C ± 0.2 K by $t = 1000$ s. This more or less amounts to a plant start-up response at half-load.
- The controller gain and integral time were set as tunable variables. The initial values used were the 'least cautious' of the manufacturers' settings.

The results were a controller gain of 0.067 K^{-1} and integral time of 65.5 s.

For a further comparison, these parameters may be compared with the classical Ziegler–Nichols tuning 'rules'[27] for a PI controller:

$$K_c = \frac{0.9\tau_p}{K_p d_p} \quad (20)$$

$$I = 3d_p \quad (21)$$

A set of open-loop plant simulations operating at the same boundary conditions as used above led to the following extrema when applying a corresponding set of 20% step changes in valve position throughout the valve range:

$4.69 \leq K_p \leq 53.65$ K

$\tau_p \cong 45$ s (all tests)

$17.4 \leq d_p \leq 30.8$ s

Thus the following Ziegler–Nichols setting were obtained:

Least cautious: $K_c = 0.49$ K^{-1}; $I = 52.2$ s

Most cautious: $K_c = 0.025$ K^{-1}; $I = 92.4$ s

The locally optimised results can be seen to lie within the Ziegler–Nichols extrema, though tending to be closer to the most cautious of these results.

6 Closed-loop plant simulation

Closed-loop plant simulations based on two of the initial manufacturers' controller settings (least cautious and most cautious) together with the optimised results from the nonlinear control design blockset are compared in Figures 11, 12 and 13. Here the plant response to a notional periodic square waveform in reference signal, r, has been generated. Figure 11 gives results at a design plant inlet air temperature of −3°C corresponding to design conditions. Figure 12 gives results at a mid-season inlet air temperature of 8.5°C, corresponding to one-half design capacity. Figure 13 gives results at a light load condition in which the plant inlet temperature is 14.25°C, corresponding to one-quarter design capacity.

As far as the manufacturers' recommendations are concerned, the least cautious settings exhibit oscillatory behaviour at all operating conditions considered, whereas the most cautious recommendations exhibit poor controlled variable tracking. Both controller specifications lack robustness in that they exhibit differing (and unsatisfactory) characteristics at each load condition. Locally optimised settings give good performance at all loads (i.e. provide robustness) but, in practice, would require on-line data from the plant or a detailed mathematical model of the plant for satisfactory tuning.

7 Conclusions

A simulation model of a discharge air temperature plant has been developed and an open-loop form of this model gives good agreement with experimental data. A limited survey of control system manufacturers has been used to obtain 'first guess' controller settings of the extensively used fixed-parameter PID controller for this type of plant. Three of the four manufacturers commented that these settings would be the subject of further adjustment on site if necessary. However, unless plant commissioning takes place at an especially nonlinear part of its operating range (e.g. light load), the need for further adjustment is uncertain in practice since commissioning may take place during conditions of favourable plant operation (e.g. near design) when the nominal manufacturers' settings might be expected to perform well. Thus the 'first guess' settings were used to obtain optimised settings at local (mid range) plant operating conditions and the optimised settings and extremes of manufacturers' settings have been used in closed-loop plant simulations. The results revealed significant deficiencies in plant robustness across a full range of operation of the plant when applying the manufacturers' settings, but the locally optimised settings give rise to considerable improvement.

Specifically:

— Least cautious 'first guess' advice from manufacturers was found to lead to very poor stability and performance characteristics by the plant.

— Most cautious 'first guess' settings were found to give stable results at design and mid-range plant loads with some instability at light load. Tracking performance was poor, especially at higher loads.

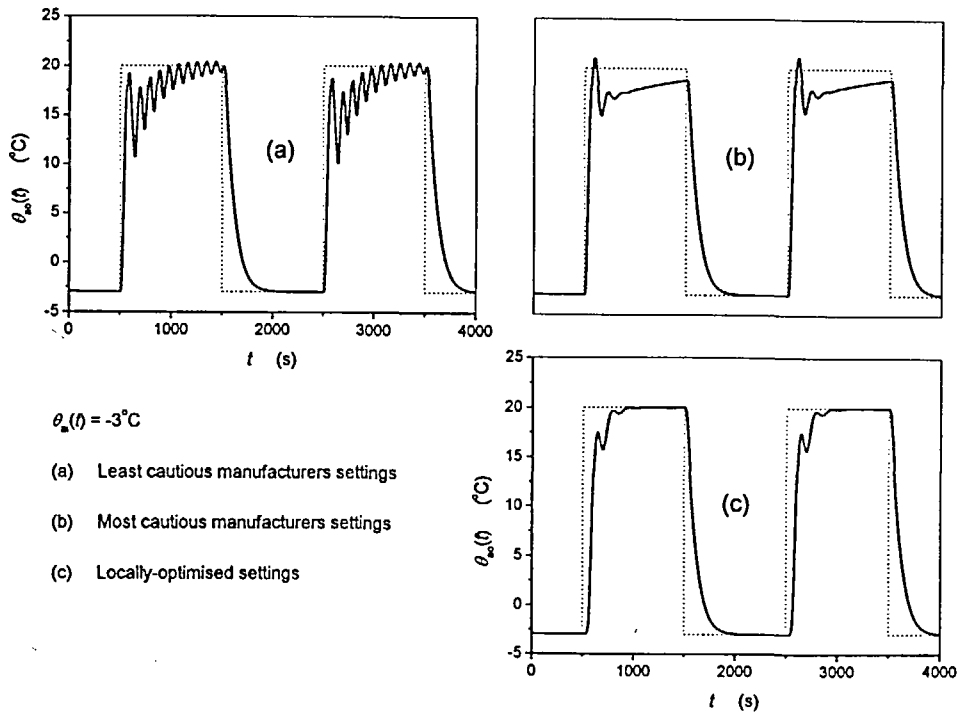

Figure 11 Closed-loop plant response at design

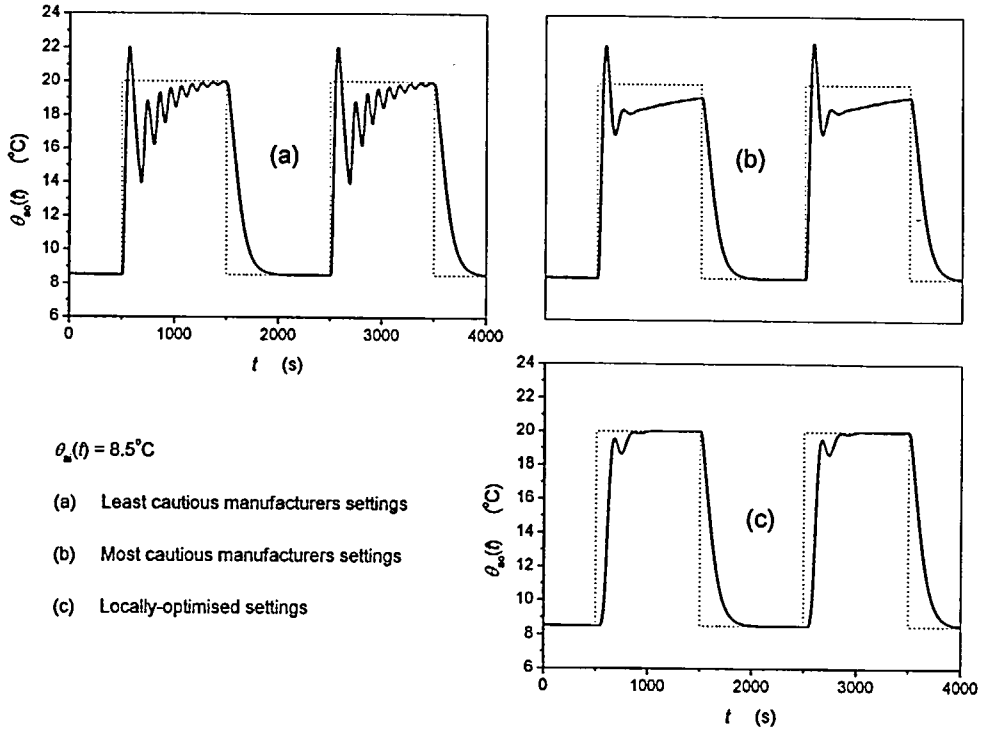

Figure 12 Closed-loop plant response at half load

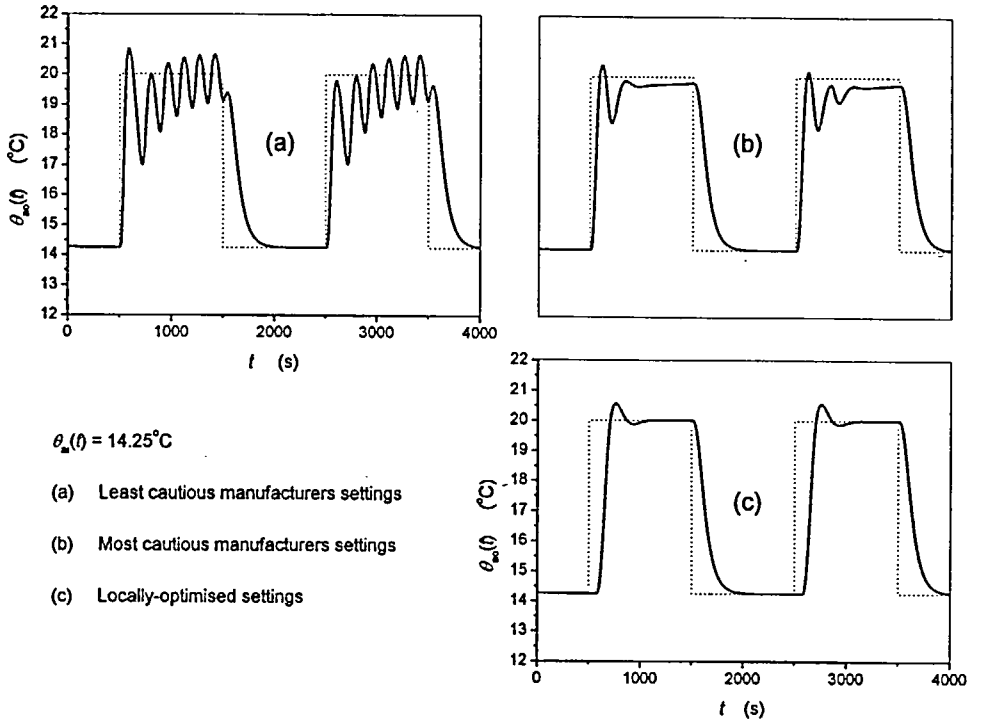

Figure 13 Closed-loop plant response at quarter load

— Locally optimised settings were found to give good stability and performance results at all load conditions but would require extensive information about plant characteristics for tuning purposes.

In Part II, the robustness issue is investigated further by considering the potential of an alternative class of fixed-parameter controllers using H^{∞} methods that offer the potential of achieving control performance that is at least as good as locally-optimised PID control, but requires limited *a priori* knowledge about the plant.

References

1 Dexter A L and Haves P A Robust self-tuning predictive controller for HVAC applications *ASHRAE Trans.* 95(2) 431–438 (1989)

2 Loveday D L, Virk G S and Cheung J M Advanced control for BEMS: a model-based predictive approach *Building Serv. Eng. Res. Technol.* 13(4) 217–233 (1992)

3 MacArthur J W and Woessner M A Receding horizon control: a model-based policy for HVAC applications *ASHRAE Trans.* 99(1) 139–148 (1993)

4 Seem J E Implementation of a new pattern recognition adaptive controller developed through optimisation *ASHRAE Trans.* 103(1) 494–506 (1997)

5 Hepworh S J, Dexter A L and Willis S T P Neural network control of a non-linear heater battery *Building Serv. Eng. Res. Technol.* **15**(3) 119–129 (1994)

6 Huang S and Nelson R M Rule development and adjustment strategies of a fuzzy logic controller for an HVAC system: Part one—Analysis and Part two—Experiment *ASHRAE Trans.* **100**(1) 841–856 (1994)

7 Curtiss P S, Kreider J F and Brandemuehl M J Adaptive control of HVAC processes using predictive neural networks *ASHRAE Trans.* **99**(1) 496–504 (1993)

8 So A T P, Chow T T, Chan W L and Tse W L A neural network-based identifier/controller for modern HVAC control *Building Serv. Eng. Res. Technol.* **101**(2) 14–31 (1995)

9 Adams S and Holmes M J *Determining time constants for heating and cooling coils* BSRIA Technical Note TN6/77 (Bracknell: Building Services Research and Information Association) (1977)

10 Gondal I A Linear analysis of an air temperature control loop *ASHRAE Trans.* **93**(2) 736–751 (1987)

11 Shavit G and Brandt S G The dynamic performance of a discharge air temperature system with PI controller *ASHRAE Trans.* **88**(2) 826–838 (1982)

12 Borresen B A HVAC control process simulation *ASHRAE Trans.* **87**(2) 871–882 (1981)

13 Brath P, Rasmussen H and Hägglund T Control of the outlet air temperature in an air handling unit *Proc. UKACC Int. Conf. CONTROL '98* (London: IEE) pp935–940 (1998)

14 Underwood D M and Crawford R R Dynamic nonlinear modelling of a hot-water-to-air heat exchanger for control applications *ASHRAE Trans.* **97**(1) 149–155 (1991)

15 Crawford R R, Dykowski R G and Czajkowski S E A separated linear least squares modelling procedure for nonlinear HVAC components *ASHRAE Trans.* **97**(2) 11–18 (1991)

16 *TRNSYS—A transient system simulation program—Volume 1 Reference manual* (Madison, WI: Solar Energy Laboratory, University of Wisconsin) (1996)

17 Clark D R *HVACSIM+ Building system and equipment simulation—Program reference manual* NBSIR 84-2996 (Gaithersberg: National Institute of Standards and Technology) (1985)

18 Underwood C P *Documentation of TRNSYS component models for HVAC applications* (University of Northumbria at Newcastle: Built Environment Research Group) (1994)

19 Dexter A L, Eftekhari M M, Haves P and Jota F G The use of dynamic simulation models to evaluate algorithms for building energy control: experience with HVACSIM+ *Proc ICBEM '87 International Congress on Building Energy Management Lausanne* (1987)

20 Metcalf R M, Taylor R D, Pedersen C O, Liesen R J and Fisher D E Incorporating a modular simulation program into a large energy analysis program: the linking of IBLAST and HVACSIM+ *Proc Building Simulation '95* (Madison, WI: International Building Performance Simulation Association) (1995)

21 *SIMULINK 2 Dynamic system simulation for MATLAB* (Natick, MA: Mathworks Inc) (1996)

22 Holman J P *Heat transfer* p 286 (New York: McGraw-Hill) (1997)

23 Rogers G F C and Mayhew Y R *Thermodynamic and transport properties of fluids* (Oxford: Basil Blackwell) (1995)

24 Ref. 22 p293 (table 6.1)

25 Gomaa A G, LeFeuvre R F, Underwood C P and Bond T J Numerical analysis of developing laminar flow and heat transfer characteristics through corrugated wall channels *Proc IMechE Heat Transfer Conference Edinburgh* paper no C565/023 pp 205–214 (1999)

26 Underwood C P and Edge J S Flow characteristics in circuits using three-port modulating control valves *Build. Serv. Eng. Res. Technol.* **16**(3) 127–132 (1995)

27 Ziegler J G and Nichols N B Optimum settings for automatic controllers *Trans. ASME* **64** 759–768 (1942)